Instrumentation Research Highlights

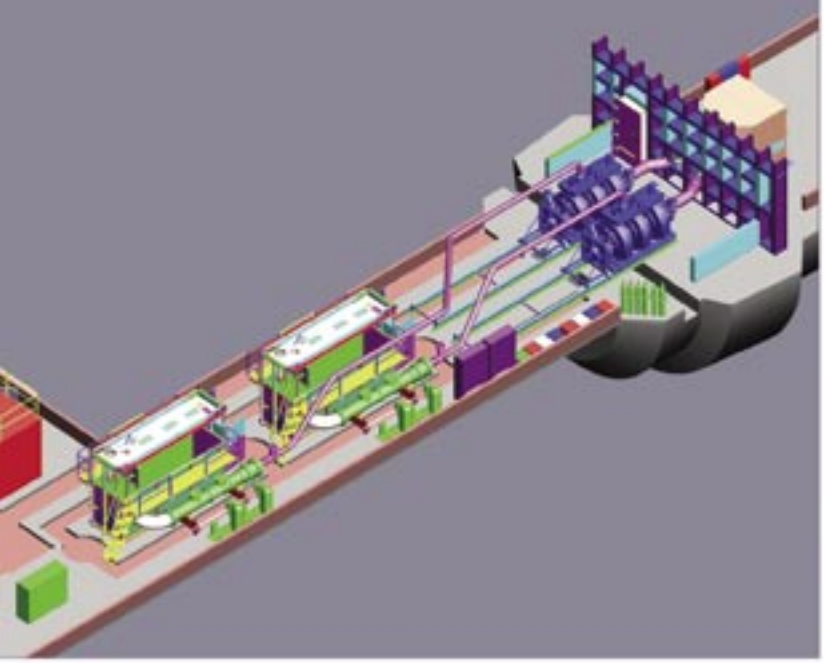

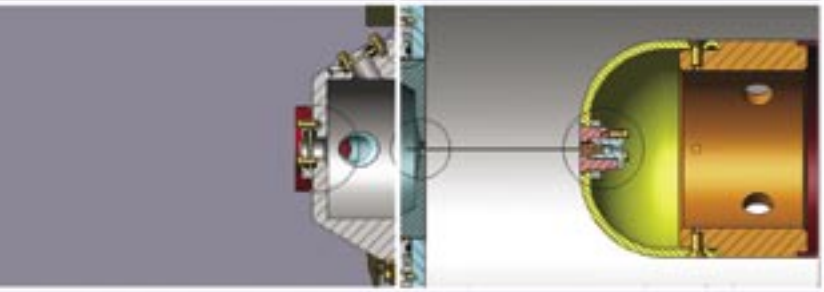

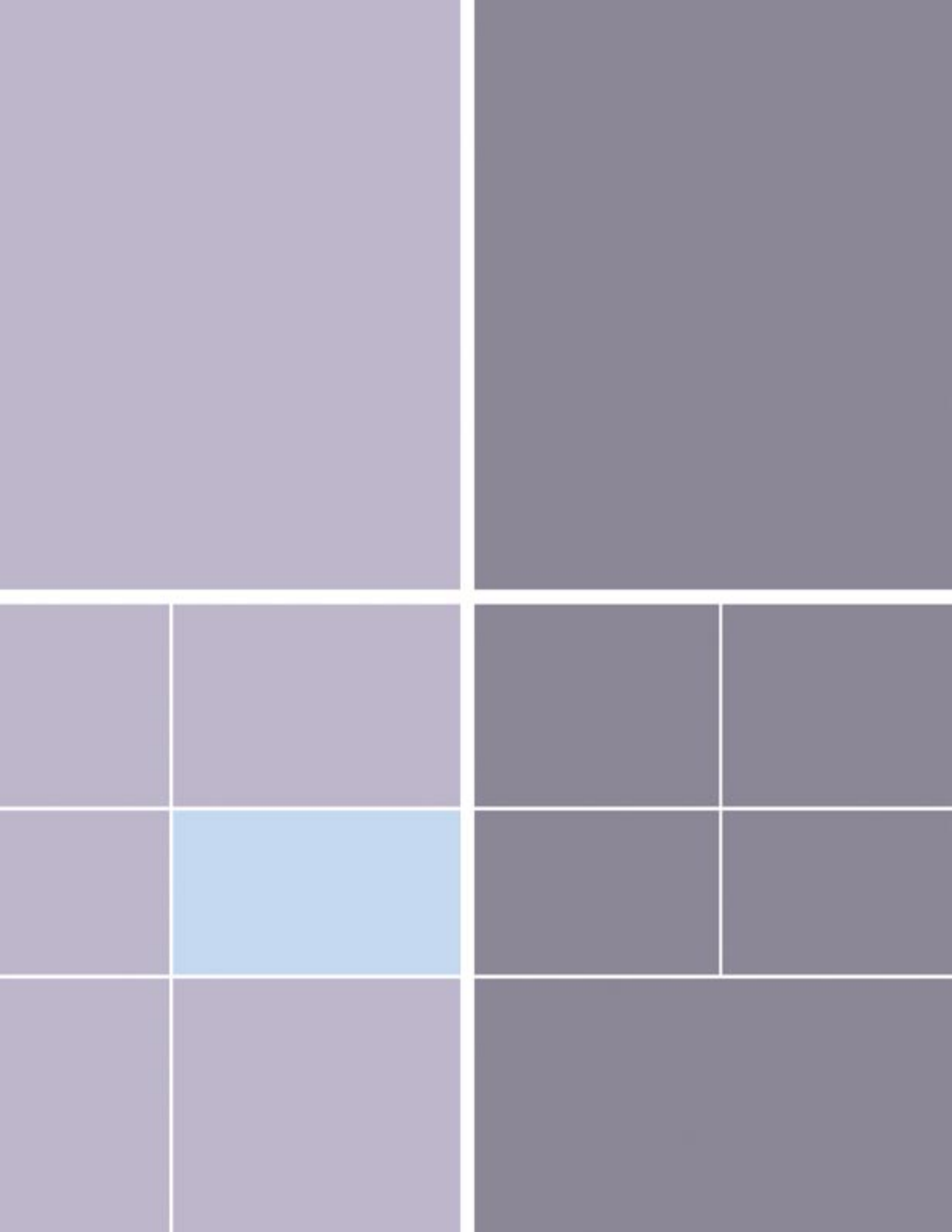

Design Feasibility and Cost Estimate for a Single-Axis, Multipulse Proton Radiography Facility

J.A. McGill, C.L. Morris (P-25), P.L. Colestock (ISR-6), F. Neri, L.J. Rybarcyk (LANSCE-1), M.E. Schulze (DX-6), H.A. Thiessen (X-4), N.S.P. King (P-23)

A recent study motivated by the success of proton radiography (pRad) experiments done at Brookhaven National Laboratory (BNL) has examined the design parameters and estimated the costs of proton synchrotrons at both 10 and 20 GeV, which can be applied to quantitative radiography for the weapons stockpile. Potential sites and capabilities at LANL or the Nevada Test Site (NTS) were studied, and design feasibility and cost estimates were completed. The goal of the study was to present options for a new hydrotest capability that provides better position resolution, a factor of 10–100 higher effective dose[1], and up to ten time frames.

The choice of the two energies is driven by the classified results of static experiments performed using 24 GeV/c and 7.5 GeV/c beams from the Alternating Gradient Synchrotron (AGS) at BNL. These experiments showed that the lower energy is sufficient for measuring weapons-physics processes in scaled experiments, which are important to certification[2]; and the higher energy is suitable for full-scale hydrotesting on the largest stockpiled systems, with significantly enhanced physics returns[3].

The Potential Sites

The prospective LANL site was selected to take advantage of the existing accelerator infrastructure at the Los Alamos Neutron Science Center (LANSCE). The 800 MeV LANSCE linear accelerator could be used as an injector, saving the time and money that would be needed to build and commission a new accelerator. In addition, the existing infrastructure of trained people and equipment would simplify commissioning a new accelerator. However, the current site-wide authorization basis would preclude using pRad to diagnose dynamic experiments with plutonium, a key requirement for certification.

The potential NTS site studied was selected to take advantage of the U1a firing site and its authorization basis for plutonium experiments. Although the underground construction required at U1a would be more expensive than the site at LANL, and an injector would have to be designed and constructed, once the machine was completed, it would be relatively straightforward to implement an authorization basis for experiments with plutonium.

The requirements for these machines were synthesized from a combination of the results from the AGS experiments and from requirements studies carried out over the last decade.[4] They are listed in Table 1.

The number of pulses is driven by the need to measure density at several times normal to infer criticality. Extensive studies by Buescher, Hopson, and Slattery have shown that four pulses spaced at a minimum of 200 ns are sufficient. We have added a fifth time to the design requirements so that early time phenomena can be studied simultaneously and critically. Up to 10 pulses can be used for the 20 GeV ring studied here, limited by the circumference of the synchrotron. The 10 GeV ring can provide up to 6 pulses at 200 ns spacing. The proton dose in Table 1 is twice what has been used in validation experiments described below. This is enough beam to allow a two-Gaussian imaging mode, in which part of the beam is used to image small radii in the object and another part of the beam is used for full-field imaging.

Table 1. Machine requirements

Number of pulses	> 5
Minimum pulse spacing	~ 200 ns
Protons per pulse	2×10^{11}
Time format	Individual pulse extraction

pRad

Transmission radiography measures the transmission of a penetrating beam through an object and uses the attenuation to measure the areal density profile (thickness) of the object. Typically, the information is used to qualitatively determine the internal structure of the object. Hydrotesting involves imploding

RESEARCH HIGHLIGHT
PHYSICS DIVISION

a primary from a weapon, in which the nuclear fuel has been replaced with a surrogate in order to not produce a nuclear yield. One goal of hydrotest radiography is to measure densities at late times in the implosion to benchmark numerical simulations that can be used to predict the explosive yield of nuclear systems. Until recently, the only diagnostic available for late-time hydrotesting was flash x-radiography.

With the cessation of underground testing, considerable effort has been expended to improve x-ray technology. The most recent manifestations of this effort are the first axis of the Dual-Axis Radiographic Hydrodynamic Test (DARHT) facility and the ARIX facility.[5] These machines produce the largest doses and smallest spot sizes ever achieved with flash x-radiography. Nevertheless, in order to answer questions about stockpile performance and long-term stockpile certification, researchers require data that flash x-radiography cannot provide.[4] Transmission radiography is described by the Beer-Lambert law.[6] The solution to the differential equation,

$$\frac{dN}{dz} = -\lambda N \text{ is } N = N_0 e^{-\frac{z}{\lambda}}, \quad (1)$$

where λ is the mean-free path of the probe, z is the distance traversed, N_0 is the incident number of particles, and N is the number surviving after a distance (z). For objects of composite materials, z/λ becomes a summation or an integral, but the analysis below remains the same. In quantitative radiography the thickness of an object can be measured as:

$$\frac{l}{\lambda} = -\ln\left(\frac{N}{N_0}\right), \quad (2)$$

where l is the total amount of material traversed. Experimentally, one must consider details that are not reflected in the above equations such as the source spectrum (because λ is a function of energy), and backgrounds, which always seem to be a problem.

In spite of the simplified treatment, it is instructive to calculate the uncertainty on the measurement of thickness Δl, under the assumption that the only source of noise is the Poisson (counting) statistics of the transmitted beam:

$$\frac{\Delta l}{\lambda} = \frac{1}{\sqrt{N}}. \quad (3)$$

The mean-free path, λ, can be chosen to minimize Δl for a given object. Setting $\frac{d(\Delta l)}{d\lambda} = 0$, and solving for $\frac{\lambda}{l}$ gives $\frac{\lambda}{l} = \frac{1}{2}$.

That is, the optimum thickness determination per unit dose occurs at twice the mean-free path. In the case of x-rays, λ is a strong function of x-ray energy. The mean-free path reaches a maximum energy value where the likelihood for pair-production (which is rising with energy) becomes comparable to Compton scattering (which is falling with energy). The maximum mean-free path is weakly dependent on z, the nuclear charge. It occurs at an energy near 4 MeV, and is about 22 gm/cm^2 or a little over a centimeter of uranium. This maximum x-ray, λ, is far from the optimum for hydrotest experiments.

An alternative is provided by hadronic rather than electromagnetic probes. The absorption cross section, σ_A, for hadrons on a nucleus with atomic number A is well-approximated by:

$$\sigma_A = \pi r_A^2, \quad (4)$$

where $r_A \approx 1.2A^{1/3}$ fm. Using $\lambda = \frac{1}{\rho\sigma_A}$ gives an estimate of the hadronic mean-free path in uranium of 220 gm/cm^2, or 11.6 cm. The tabulated value is 199 gm/cm^2.[7] Measurement of thickness is optimized at around 23 cm of uranium. This is much better matched to hydrotest radiography than the x-ray mean-free path. Consequently, the same statistical information can be obtained with a much lower incident flux of hadrons than with high-energy x-rays.

Advantages of pRad

It is possible to take advantage of the long hadronic mean-free path by using high-energy protons as a radiographic probe. High intensities are available in short pulses using current accelerator technology. Because the protons are charged, a proton beam can be distributed across a radiographic object and focused onto downstream detectors using electromagnets.[8]

In a set of experiments performed using the AGS at BNL, data were taken on a set of test objects to validate pRad and to compare it to x-radiography from DARHT. In all cases that have been studied, the qualities expected from pRad have been verified, and in all comparisons, even modest pulses of 10^{10} protons have been observed to provide a radiographic advantage over DARHT performance by a factor of between 10 and 100 in units of dose.

Even more significantly, pRad has been demonstrated to be quantitative at the percent level, and in high-fidelity mockups of hydrotest experiments, pRad demonstrates the capability to measure some of the underlying physics of cavity shape and mix, topics that have been identified as requirement drivers for hydrotest radiography.

The costs are based on a model developed in the Advanced Hydrotest Facility (AHF) project, and are expected to be accurate to ± 20%. It must be emphasized that this study is intended only to show the outlines of a facility that would provide the high-quality radiography discussed above and a rough cost estimate for such a facility. A more definitive design and estimate will be produced during conceptual design.

Scope and Cost

The goals of the accelerator complex are to satisfy the parameters in Table 1. The most demanding machine is the 20 GeV main ring synchrotron, common to both the LANL and the NTS sites. The alternative, a 10 GeV ring, has been studied only to

Table 2. Parameters of the strawman 20 GeV lattice

Circumference	608 m
Number of Dipoles	56
Dipole length, field, gap	5.0 m., 1.56 T, 5 cm
Number of Quads	76
Quad length, Gradient, aperture	0.8 m., 11.3 T/m, 10 cm
Transition gamma	5.73
Admittance (normalized)	16 π mm-mr

Table 3. Parameters for the 10 GeV Ring

Circumference	392 m
Number of Dipoles	40
Dipole length, field, gap	4.0 m., 1.43 T, 5 cm
Number of Quads	56
Quad length, Gradient, aperture	0.6 m., 8.5 T/m, 10 cm
Transition gamma	4.22
Admittance (normalized)	16 π mm-mr

the level of detail necessary to show its proof of principle. Capture, ramp, and acceleration have been studied for the 20 GeV ring, assuming injection could be provided by LANSCE's 800 MeV linac, or from the 500 MeV "green-field" injection complex at NTS. Detailed studies of the dynamics in the 10 GeV machine have only been done assuming injection from the LANSCE linac.

A 500 MeV booster synchrotron injects the larger machine (either 10 or 20 GeV) for the NTS siting option. The booster is injected by a small commercially available 11 MeV H(-) linac. As with the larger machines, the dynamics of the booster have been studied to such detail that its final design can be bounded, and to provide a reasonable estimate of its cost.

The overall layout of the ring is a racetrack design as shown in Figure 1. The pair of long straight sections provide for injection, extraction, and acceleration. Parameters of the Main Ring are in Table 2. The 10 GeV design is conceptually similar to the 20 GeV design, and results in an overall smaller circumference (Figure 2). The reduction in size is not precisely a factor of two from the 20 GeV case owing to the required straight sections and other infrastructure for injection and extraction. The ring's parameters are given in Table 3. The accelerators proposed here are well within the parameters of other accelerator projects that have been proposed and/or built. The reported (or estimated) costs of these accelerators vary considerably from site to site; nevertheless a reasonable estimate can be made, accurate to probably 20%. The costs of several synchrotron projects were studied in the AHF project. Those costs were summarized and reported by Prichard[9] and incorporated into a model for costing synchrotrons. The model uses gross measures, such as total weight of dipole and quadrupole magnets, total amount of direct-current power, total length of beampipe vacuum, etc. Cost rates are applied to generate a total equipment cost. Factors are applied for overheads, design costs, and contingency, to arrive at the total project cost (TPC) for the accelerator equipment. A similar breakdown is done for the balance of plant, and cost loading factors specific to the civil construction process is applied. The result of the two exercises is an estimated TPC.

References

1. C.L. Morris *et al.,* to be published in DDR 2003.
2. S. Sterbenz *et al.,* Nuclear Explosives Design Physics Conference, Los Alamos, 2003
3. C.L. Morris *et al.,* to be published in DDR 2003.
4. J. Hopson, K. Buescher, and W. Slattery have done extensive work on establishing and quantifying a criticality requirement.
5. C. Ekdahl, "Modern Electron Accelerators for Radiography," *IEEE Transactions on Plasma Science,* **30** 254–261 (2002).

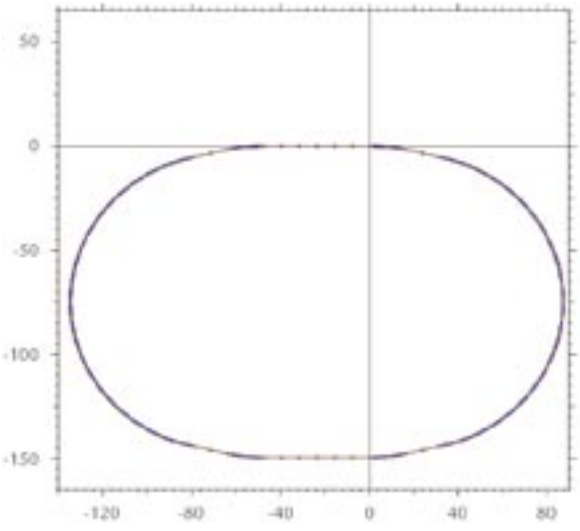

Figure 1. Concept for a 20 GeV ring design. The design is composed of two circular arcs coupled by matching sections into straight sections.

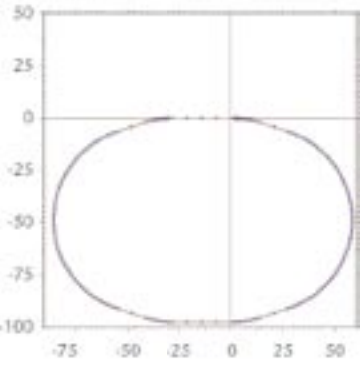

Figure 2. Concept for a 10 GeV ring design similar to that of the 20 GeV ring, but with a shorter circumference.

6. A. Beer, *Annals der Physik Chemie* **86**, 78 (1952).
7. Particle Data Group, *The European Physical Journal C* **v3**, 1 (1998).
8. A. Gavron *et al.,* "Proton radiography," Los Alamos National Laboratory document LA-UR-96-420.
9. B. Prichard, AHF Tech. Note 619, *A costing formula for proton synchrotrons,* 2003.

Acknowledgment

For further information, contact Chris Morris, 505-667-5652, cmorris@lanl.gov.

Table 4. Summary of costs for the various options

	20 GeV Ring		10 GeV Ring	
Cost Element	**NTS**	**LANL**	**NTS**	**LANL**
Equipment				
Linac	$7.8		$7.8	
Booster	$16.2		$16.2	
Main Ring	$64.7	$64.7	$45.2	$45.2
Transfer Lines	$3.4	$7.4	$3.4	$7.4
Firing Site & Detectors	$7.6	$7.6	$7.6	$7.6
Balance of Plant	$260.2	$83.7	$225.1	$69.0
Total	**$ 359.9**	**$ 163.4**	**$ 305.3**	**$ 129.2**

Costs are in $M, FY07, The NTS costs have been validated by independent estimates made by Bechtel Nevada.

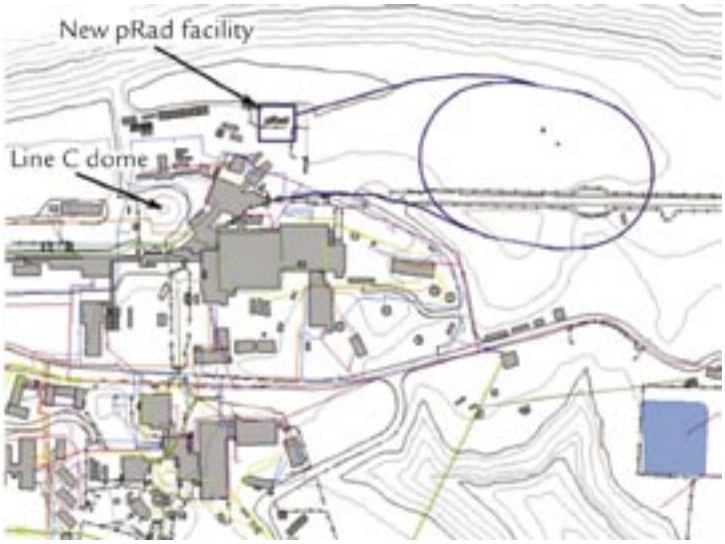

Figure 3. A possible site for the 20 GeV ring, shown overlaid on the LANL Technical Area 53 site.

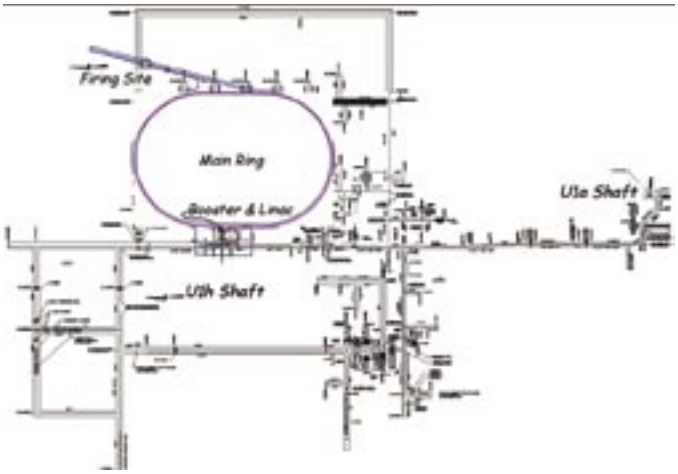

Figure 4. A possible layout of the accelerator complex, overlaid on the NTS U1a complex. There are no pre-existing facilities at the NTS to work around, so the accelerators and firing site can be positioned next to each other (allowing for operational considerations).

Cygnus—A New Radiographic Diagnostic for Subcritical Experiments

J.R. Smith, R.L. Carlson (P-22), R.D. Fulton (P-23), J.R. Chavez, P.A. Ortega, R.G. O'Rear, R.J. Quicksilver (DX-3), B. Anderson, D.J. Henderson, C.V. Mitton, R. Owens (BN), S. Cordova, J.E. Maenchen, I. Molina, D. Nelson, E. Ormond (SNL)

The subcritical experiment (SCE) program was initiated after the 1992 moratorium on underground nuclear testing in support of stockpile stewardship.[1] The dynamic material properties of plutonium are a major topic of exploration for the SCE program. In order to provide for a multilayered containment of plutonium, the SCEs are executed in the U1a underground tunnel complex at the Nevada Test Site (NTS). We developed Cygnus, a new radiographic x-ray source, for diagnostic support of the SCE program at NTS. We took the name Cygnus from the binary star Cygnus X-1, located in the constellation Cygnus, which is a strong x-ray source. For the special conditions related to this application, we emphasize design in areas affecting machine placement, remote operation, and reliability.

Typically, SCEs have been limited to surface diagnostics such as interferometry and pyrometry. The interferometry system commonly used on SCEs is called VISAR (velocity interferometer system for any reflector). We developed x-ray radiography to complement the existing surface diagnostics, provide a more extensive spatial view (albeit temporally limited), and provide internal (penetrating) measurements. The Stallion series of SCEs consists of four shots: Vito, Rocco, Mario, and Armando.[2] Armando was the initial experiment for Cygnus radiography. The Rocco, Mario, and Armando tests use identical physics packages, permitting the use of Armando radiographic results as a confirmation of VISAR measurements. The main x-ray source requirements for an SCE involve spot size, intensity, penetration, and duration. The Cygnus source meets the following design specifications: ~ 1 mm diameter, 4 Rads dose at a distance of 1 m, ~ 2.25 MeV endpoint energy, and < 100 ns pulse length. Two Cygnus sources (Cygnus 1, Cygnus 2) were fielded on Armando providing two radiographic views separated in space by 60° and in time by 2 μs.

Cygnus Design and Layout

A multiorganizational team (LANL, Bechtel Nevada, Sandia National Laboratories, Naval Research Laboratory, and Titan/Pulse Sciences Division [Titan/PSD]) was formed to design a prototype x-ray machine in response to the programmatic need for fielding a radiographic diagnostic on SCEs. The design concept is based on three criteria:

(1) it must fulfill the radiographic source requirements as previously stated;

(2) it must accommodate the U1a tunnel environment in terms of footprint, operations, and safety; and

(3) it must be reliable.

To satisfy the first criterion, the key is use of the rod-pinch diode that is a low-impedance, high-dose diode.[3] This approach yields a smaller source size in comparison with other diode types. We met the footprint component of the second criterion by using a modular pulsed-power design where the energy storage unit (Marx) is independently located with respect to the inductive voltage adder (IVA), which are both connected by a coaxial water-transmission line. We achieved the reliability criterion by using proven pulsed power elements, extraordinarily conservative mechanical and pulsed-power designs, and an extensive test program.

The overall Cygnus layout in Figure 1 shows the two sources as fielded at NTS/U1a. Proceeding downstream, the major elements are: Marx generator, pulse-forming line, water-transmission line, IVA, and rod-pinch diode. Not shown is the high-voltage trigger generator used to initiate the Marx pulse. Titan/PSD integrated these pulsed-power elements into a design for the Cygnus system.[4]

Cygnus Test Plan and Deployment

Cygnus Prototype Tests at LANL. The "demonstration test" for Cygnus was performed at LANL. This test involves assembly of a prototype machine and testing via a series of shots designed to prove that the Cygnus design would meet or exceed x-ray source requirements

(diameter, dose, endpoint energy, and pulse length), as well as operational requirements (reliability, reproducibility). A total of 118 protype test shots were completed.

Shot analysis shows design specifications for the source were met or exceeded.[5] Successfully demonstrating that the prototype machine meets all design criteria and provides an acceptable level of reliability, we proceeded with the project along the following paths:

(1) Promotion of the existing machine from prototype to field status (i.e., a source suitable for use on a SCE shot) and designation as Cygnus 1. Relocation of Cygnus 1 to a LANL firing site (R-306) for extended testing.

(2) Approval of fabrication and testing of a second source (Cygnus 2) at Titan/PSD.

Cygnus 1 Field Tests at LANL. Cygnus 1 was moved to the LANL firing site for the extended testing phase. At this site, a structure was built to replicate underground installation at U1a for the express purpose of certifying the instrument in a realistic environment. Matching R-306 and U1a features include: wall and ceiling dimensions; bulkhead wall construction; electrical-utility placement; and installation of a camera house, camera monitoring system, and a remote control system. We completed 202 shots at R-306.

The R-306 tests show that Cygnus 1 was suitable for installation and operation in the U1a environment, did not produce levels of radiation adverse for operation of other planned diagnostics or systems, and produced images with the desired spatial quality and intensity. Therefore, Cygnus 1 was approved for underground installation at U1a.

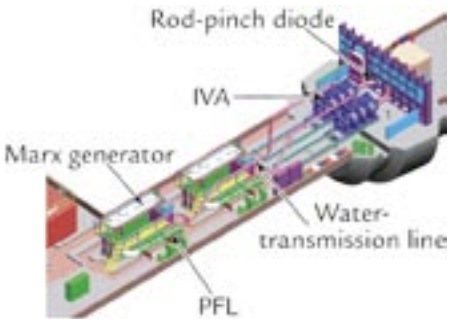

Figure 1. Cygnus 1 and 2 as fielded at NTS/U1a.

Cygnus 2 Construction at Titan/PSD. Titan/PSD was contracted to deliver a second machine, Cygnus 2, which is similar to Cygnus 1 with the exception of a longer coaxial transmission line. Assembly and testing of Cygnus 2 paralleled with testing of Cygnus 1 at R-306. Testing at PSD consisted of 410 shots. Cygnus 2's performance during the acceptance tests was similar to that of Cygnus 1, and the machine was ultimately approved for installation at U1a.[6]

Cygnus 1/Cygnus 2 Deployment at NTS/U1a. Figure 1 shows Cygnus 1 and 2 in the U1a.05 drift. Note that placing the Marx tanks end-to-end and the IVAs side-to-side accommodates the tunnel dimensions. The rod-pinch diodes are oriented with a 60° included angle. A bulkhead containment wall separates the zero room, which houses the experiment, from the Cygnus machine area. The test object is contained in a 3 ft diam vessel, thereby permitting reuse of the zero room. The camera system is protected in a camera room that has 1 in. thick steel walls. Tungsten collimators are placed in the bulkhead wall and camera room wall to reduce image "noise" from scattered x-rays. Both Cygnus machines may be monitored and controlled either from a screen room located in the .05A drift alcove, or from a diagnostic trailer on the surface. A total of 237 shots, the sum of shots from both machines, were fired at U1a.

Table 1 gives a breakdown of the number of shots completed for each facility as well as for each source. The total shot number (967) is an indication of the considerable effort given in this endeavor.

Cygnus Reliability is a Key Operational Element

The risk inherent in the execution of a SCE is that a high-stakes package is expended in a single event where there is no reprieve from equipment failure. In this respect, an SCE is similar to a NASA rocket launch. On command, Cygnus must reliably deliver x-rays at a specified time. Because Cygnus radiography is the primary diagnostic for Armando, and therefore a key metric for its success, pressure to guarantee high reliability was intense. We were especially concerned with two catastrophic failure modes for Cygnus that would result in losing the radiographic image. Just as in the rocket-launch scenario, a critical time in the SCE countdown specifies a "point of no return" where the event cannot be stopped. Both Cygnus failure modes correspond to malfunctions that occur after this critical time. The first failure mode is due to either a trigger

Table 1. Cygnus shot record

	LANL TA-3/SM-316				LANL TA-15/R-306				Titan/0PSD				NTS/U1a				Total
	MRX	PFL	LAD	RPD	MRX	PFL	LAD	RPD	MRX	PFL	LAD	RPD	MRX	PFL	LAD	RPD	
Cygnus 1	5	7	46	60	31	0	102	69					54	0	11	58	443
Cygnus 2									85	217	108	0	52	0	16	46	524
Total	118				202				410				237				967

The four shot modes are:
MRX = Marx resistive load
PFL = pulse-forming-lines resistive load
LAD = large-area ciode
RPD = rod-pinch diode

Figure 2. Thermoluminescent dosimetry results for Cygnus 1 and 2 at U1a. Note, shot #100 is the confirmatory shot, and shot #144 is the Armando shot.

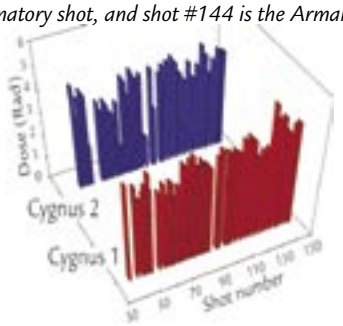

generator or Marx generator *prefire,* resulting in premature radiation. The second failure mode is a *no-fire* situation, where the Marx fails to breakdown on command due to either a trigger failure or Marx failure, resulting in no radiation.

The three provisions below were implemented to enhance the probability for success.

Readiness. Historically, the Cygnus trigger generator and Marx generator components have exhibited a tendency for failure. In order to check these components, as well as the control and data acquisition systems, we instituted a preliminary shot procedure. This involves firing a dual-resistive load shot approximately 15 to 30 minutes before the planned radiography shot. This procedure is very effective in discovering preshot personnel error or equipment failure and in assuring system readiness.

Prefire Protection. Although we thought that trigger-generator problems previously discovered during prototype tests were fixed, initially there were frequent trigger-generator prefires on both Cygnus machines at U1a. As a result, we sent the trigger generators to LANL for extensive evaluation, testing, and modification to remedy the problem. We implemented an additional level of precaution to prevent prefire: we turned on the trigger generator high-voltage power supply just before a shot (~ 10 s). This method minimized the exposure to prefire and worked well even with trigger generators prone to prefire. Dirty spark gaps, as was discovered early in the program, encourage Marx generator prefire. Spark-gap purging is included as a command in the control software. It is done liberally (i.e., with significant gas flow) and often. Several Marx generator prefires occurred on Cygnus 1 just before the confirmatory shot. After the confirmatory shot, an inspection revealed the cause as several broken trigger resistors. After replacing the resistors, and during the period between the confirmatory shot (#100) and the Armando shot (#144), neither Cygnus machine experienced trigger-generator or Marx-generator prefires.

No-Fire Protection. Marx no-fires are typically caused by spark gap overpressure. Too much pressure leads to a no-fire, while too little pressure yields prefires. The Cygnus Marx pressures were set to favor the prefire case because there are no timely warnings for a no-fire, while the prefire has a good probability of occurrence before the critical time where the shot can be "saved." We observed zero no-fire events on either machine.

Cygnus Reproducibility is a Key Operational Element

Shot-to-shot reproducibility of x-ray parameters is an important demonstration that source quality is consistent and that good radiography performance will likely be delivered on the Armando shot. It is also important because reproducible shots are required to baseline other diagnostic systems (e.g., to produce a repeatable electromagnetic interference background) and adjust the camera imaging system (e.g., alignment, intensity).

Dose results for U1a shots are shown in Figure 2. The gaps in the data primarily represent nonradiation shots, either the Marx resistive load or large area diode test modes. The low-dose shots, most predominantly seen on Cygnus 2, were caused by alignment or vacuum problems in the diode. These problems had been fully addressed by the day of the confirmation shot.

The average dose for all rod-pinch shots in the time period from the confirmation shot to the Armando shot is: 4.4 ± 0.5 Rad

Figure 3. Diode voltage, diode current, and x-ray waveforms for the Armando shot #144.

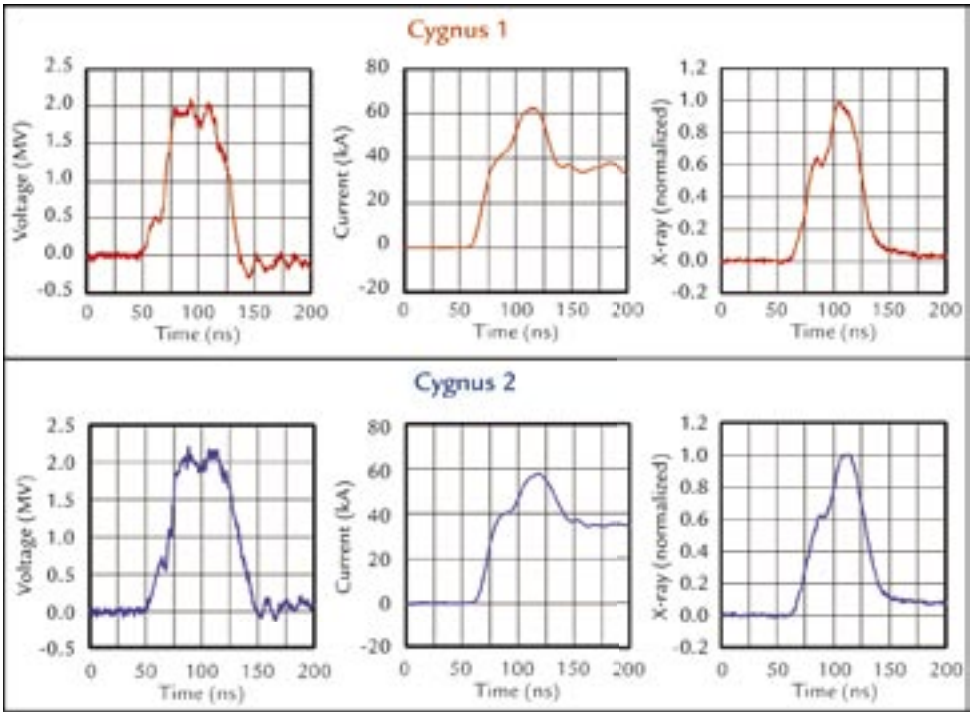

(Cygnus 1) and 4.1 ± 0.4 Rad (Cygnus 2). These measurements are standardized for a source-detector distance of 1 m, and for attenuation through 1 in. thick aluminum. Endpoint voltage is an indication of source penetration. The endpoint voltage for the same database as cited above is: 2.1 ± 0.1 MV (Cygnus 1) and 2.3 ± 0.1 MV (Cygnus 2). Reproducibility in Cygnus source intensity and penetration, shown by the standard deviation in dose and endpoint voltage above, easily satisfies the desired shot-to-shot performance.

Table 2. Armando shot summary

Shot #144	Cygnus Diode		Electrons		X-rays	
	Endpoint Voltage (MV)	Average Impedance (W)	Total # ($x10^{16}$)	Average Energy (MeV)	Dose (Rad)	Pulse Length (ns)
Cygnus 1	2.1	38	2.2	1.5	4.5	47
Cygnus 2	2.2	42	2.1	1.6	4.2	48

Conclusion—Cygnus Succeeds on the Armando SCE

The Armando shot was executed on May 25, 2004. The efforts of more than three years of planning and testing are encompassed in Cygnus performance on this single shot. It is, therefore, appropriate to conclude by presenting Armando results. Diode voltage, diode current, and x-ray waveforms (Figure 3) are key indicators of Cygnus performance. By visual comparison of the Cygnus 1 and 2 waveforms, it is evident that both machines produced markedly similar results. Several quantitative measurements of Cygnus performance on the Armando shot are given in Table 2. The measurements are placed in three categories representing different facets of machine output: Cygnus diode, electrons, and x-rays. On the Armando shot, Cygnus 1 (Cygnus 2) satisfied source requirements as follows: ~ 1mm x-ray source diameter, 4.5 (4.2) Rad dose, 2.1 (2.2) MeV endpoint energy, and 47 (48) ns pulse length. Additionally, the desired timing with a pulse separation of 2 μs was delivered. The success of Cygnus at U1a is a historical milestone that demonstrates the feasibility of fielding large and complex diagnostic systems downhole. Its success paves the way for Cygnus participation in future SCEs as well as promotes consideration of even larger radiographic facilities at U1a.

References

1. L.R. Veeser *et al.,* "Subcritical plutonium experiments at the Nevada Test Site," *1997–1998 Physics Division Progress Report,* Los Alamos National Laboratory report LA-13606-PR (May 1999) pp. 94–101.
2. D. Fulton, M.D. Wilke, and N.S.P. King, "Dynamic material studies in subcritical experiments: Rocco, Mario, Vito, and Armando," *Physics Division Activity Report,* Los Alamos National Laboratory report LA-14112-PR (February 2003) pp. 23–26.
3. G. Cooperstein *et al.,* "Theoretical modeling and experimental characterization of a rod-pinch diode," *Physics of Plasmas* **8**, 4618–4636 (2001).
4. D. Weidenheimer *et al.,* "Design of a driver for the Cygnus x-ray source," *Proceedings of the 13th IEEE International Pulsed Power Conference,* R. Reinovsky, M. Newton, Eds. (IEEE, Piscataway, New Jersey, 2001), Vol. (1) pp. 591–595.
5. J.R. Smith *et al.,* "Performance of the Cygnus x-ray source," *Proceedings of the 14th International Conference on High Power Particle Beams,* TA. Melhorn, M.A Sweeney, Eds. (AIP, Melville, New York, 2002), Vol. (1), pp. 135–138.
6. V. Carboni *et al.,* "Pulse power performance of the Cygnus 1 and 2 radiographic sources," *Proceedings of the 14th IEEE International Pulsed Power Conference,* M. Giesselmann, A. Neuber, Eds. (IEEE, Piscataway, New Jersey, 2003), Vol. (2) pp. 905–908.

Acknowledgment

We gratefully acknowledge support for this work from many colleagues in Physics and Dynamic Experimentation Divisions at LANL, and from colleagues at Bechtel Nevada, Sandia National Laboratories, Titan/PSD, and Naval Research Laboratory. Special recognition is given for Nevada Operations and Bechtel Nevada support at NTS which was instrumental in fielding Cygnus at U1a. This work was sponsored by the U.S. DOE.

For further information, contact John R. Smith, 505-665-8546, smith@lanl.gov.